NIH Public Access
Author Manuscript
Circ Cardiovasc Imaging. Author manuscript; available in PMC 2011 September 1.

Published in final edited form as:
Circ Cardiovasc Imaging. 2010 September 1; 3(5): 550–558. doi:10.1161/CIRCIMAGING.109.918540.

A Novel Approach to Early Detection of Doxorubicin Cardiotoxicity using Gadolinium Enhanced Cardiovascular Magnetic Resonance Imaging in an Experimental Model

James C. Lightfoot, MD[3], **Ralph B. D'Agostino Jr, PhD**[5], **Craig A Hamilton, PhD**[1], **Jennifer Jordan, BS**[1], **Frank M. Torti, MD**[4], **Nancy D. Kock, DVM, PhD**[2], **James Jordan, PhD**[7], **Susan Workman**[3], and **W Gregory Hundley, MD**[3,6]

[1]Department of Biomedical Engineering, at the Wake Forest University School of Medicine, Medical Center Boulevard, Winston-Salem, North Carolina, USA

[2]Department of Comparative Medicine, at the Wake Forest University School of Medicine, Medical Center Boulevard, Winston-Salem, North Carolina, USA

[3]Department of Internal Medicine, Cardiology Section, at the Wake Forest University School of Medicine, Medical Center Boulevard, Winston-Salem, North Carolina, USA

[4]Department of Internal Medicine, Hematology and Oncology Section, at the Wake Forest University School of Medicine, Medical Center Boulevard, Winston-Salem, North Carolina, USA

[5]Department of Public Health Sciences, at the Wake Forest University School of Medicine, Medical Center Boulevard, Winston-Salem, North Carolina, USA

[6]Department of Radiology, at the Wake Forest University School of Medicine, Medical Center Boulevard, Winston-Salem, North Carolina, USA

[7]Department of Cardiothoracic Surgery at the Wake Forest University School of Medicine, Medical Center Boulevard, Winston-Salem, North Carolina, USA

Abstract

Background—To determine if cardiovascular magnetic resonance (CMR) measures of gadolinium (Gd) signal intensity (SI) within the left ventricular (LV) myocardium are associated with future changes in LV ejection fraction (LVEF) after receipt of doxorubicin (DOX).

Methods and Results—Forty Sprague-Dawley rats were divided into 3 groups scheduled to receive weekly intravenous doses of: normal saline (NS) (n=7), 1.5 mg/kg DOX (n=19), or 2.5 mg/kg DOX (n=14). MR determinations of LVEF and myocardial Gd-SI were performed before and then at 2, 4, 7, and 10 weeks after DOX initiation. During treatment, animals were sacrificed at different time points so that histopathological assessments of the LV myocardium could be obtained. Within group analyses were performed to examine time-dependent relationships

Correspondence to: W. Gregory Hundley, MD Cardiology Section Wake Forest University Health Sciences Medical Center Boulevard Winston-Salem, North Carolina 27157-1045 Phone: (336) 716-0607 Fax: (336) 713-0163 ghundley@wfubmc.edu.

Subject Codes: [124] Cardiovascular imaging agents/Techniques; [130] Animal models of human disease

Disclosures
None.

Publisher's Disclaimer: This is a PDF file of an unedited manuscript that has been accepted for publication. As a service to our customers we are providing this early version of the manuscript. The manuscript will undergo copyediting, typesetting, and review of the resulting proof before it is published in its final citable form. Please note that during the production process errors may be discovered which could affect the content, and all legal disclaimers that apply to the journal pertain.

NIH-PA Author Manuscript
NIH-PA Author Manuscript
NIH-PA Author Manuscript

NIH-PA Author Manuscript

NIH-PA Author Manuscript

NIH-PA Author Manuscript

between Gd-SI and primary events (a deterioration in LVEF or an unanticipated death). Six of 19 animals receiving 1.5 mg/kg of DOX and 10/14 animals receiving 2.5 mg/kg of DOX experienced a primary event; no NS animals experienced a primary event. In animals with a primary event, histopathological evidence of myocellular vacuolization occurred (p=0.04), and the Gd-SI was elevated relative to baseline at the time of the event (p<0.0001) and during the measurement period prior to the event (p=0.0001). In all animals (including NS) without an event, measures of Gd-SI did not differ from baseline.

Conclusions—After DOX, low serial measures of Gd-SI predict an absence of a LVEF drop or unanticipated death. An increase in Gd-SI after DOX forecasts a subsequent drop in LVEF as well as histopathologic evidence of intracellular vacuolization consistent with DOX cardiotoxicity.

Keywords

cardiotoxicity; chemotherapy; congestive heart failure; doxorubicin

Doxorubicin (DOX) is an important drug in modern therapy for breast cancer, soft tissue sarcomas, acute leukemia, Hodgkin's and non-Hodgkin's lymphoma, and many childhood cancers.[1] Unfortunately, the use of DOX, as well as other anthracyclines, is limited by cardiotoxicity that precipitates congestive heart failure (CHF).[2]

DOX-induced cardiomyopathy is difficult to detect. Serial measures of left ventricular ejection fraction (LVEF) with radionuclide ventriculography or transthoracic echocardiography are often used screen cancer patients for irreversible cardiotoxicity and CHF, but an observed drop in LVEF often occurs too late to avert irreversible cardiomyopathy.[2-5] Also, current clinical surveillance imaging strategies do not identify early myocellular evidence of DOX cardiotoxicity.

Cardiovascular magnetic resonance (CMR) imaging can be used to characterize myocardial tissue, and identify myocardial necrosis and fibrosis without exposure to ionizing radiation or radioisotopes.[6] This study was performed in animals receiving DOX to determine if changes in gadolinium (Gd) signal intensity (SI) on T1-weighted CMR images would forecast a future drop (or preservation) of LVEF, or histopathologic findings indicative of myocardial injury, necrosis, or fibrosis.

Methods

Study design

This study was conducted at the Wake Forest University School of Medicine as part of a protocol approved by the Animal Care and Use Committee and funded by the National Institute of Health (study identifier: R21CA109224). A total of 40 Sprague-Dawley male rats (weighing 250 to 350 g) were enrolled into 1 of 3 groups. The first group of animals (n=7) received a weekly dose of intravenously administered normal saline (NS). The second group of animals (n=19) received an intermediate dose (1.5 mg/kg/week) of DOX administered intravenously by tail vein. The third group of animals (n=14) were administered a higher dose (2.5 mg/kg/week) of DOX by tail vein. Doses were selected to mimic low and high dose strategies used in clinical chemotherapy regimens. All animals were fed a standard rat chow and allowed free access to water.

Animals were scheduled to undergo CMR examinations at baseline and then again at 2, 4, 7, and 10 weeks after weekly receipt of DOX or NS. At the 2, 4, 7, and 10 week intervals, a random set of animals were withdrawn from the cohort for necropsy with histopathologic examination of the heart. During treatment, observations on body condition were made

NIH-PA Author Manuscript

NIH-PA Author Manuscript

NIH-PA Author Manuscript

throughout the experiment (Table 1). Also, animals with adverse appearance (and near expected death) were sacrificed prior to death.

The primary outcome in this study was predefined as one of 3 conditions including: a drop in LVEF of >10% from the resting baseline value at a subsequent measurement; if the absolute level of LVEF dropped below 65% at any time; or an animal died unexpectedly. These metrics were selected to be similar to clinical standards used in humans for identifying individuals at risk of DOX cardiotoxicity. Comparisons were performed between CMR measures of LVEF and Gd-SI, histopathologic findings, and the primary outcome.

CMR Technique

Scans were obtained using a 1.5 Tesla scanner equipped with a small phased-array surface coil wrapped around the animals to enhance signal to noise. Images were collected using cardiac gating obtained from electrocardiographic leads attached bilaterally to the paws. Inhalational isoflurane, 0.0004 mg/g of intramuscular (IM) ketamine, and 0.004 mg/g of IM xylazine were used for anesthesia during the CMR acquisitions. After each CMR procedure, the animals were recovered under a warm light to preserve body heat.

According to previously published methods, cine white blood, steady-state free-precession images were collected for measuring LV volumes and EF.[7] These sequences were placed along the long axis of the left ventricle as a series of 3 mm thick mid-short axis slices separated by a 3 mm gap. Imaging parameters for these sequences included an 8.3 ms repetition time (TR), a 3.0 ms echo time (TE), a 6 cm field of view (FOV), a 256×256 matrix, and a 30 degree flip angle. Calculation of LV volume was performed according to previously published techniques by summing the endocardial area within each slice and multiplying by the slice thickness.[7-10] To determine LVEF, the LV stroke volume was acquired by subtracting the LV end-diastolic volume from the end-systolic volume and then dividing by the end-diastolic volume.[8]

Determination of Gd signal characteristics

Animals were injected intravenously via the tail vein with 0.2 mm/kg of gadoteridol (ProHance Bracco Diagnosis Princeton NJ); the time of this injection was recorded. Twenty minutes from the time of contrast injection, a middle LV short axis plane was acquired using a fast gradient echo sequence incorporating a non-selective inversion pre-pulse.[11] This slice was positioned perpendicularly across the middle left ventricle 6 mm from the LV apex at the midpapillary muscle level (Figure 1). This particular image acquisition slice corresponded to the slice position used later for histopathologic sectioning. The imaging strategy in this study was selected to detect myocardial fibrosis in the mid-wall of the left ventricle. The CMR parameters for observing Gd-SI included a GEIR image with a 6 ms TR, a 2 ms TE, a 6 cm FOV, a 256×256 matrix, and a 3 mm slice thickness with an inversion delay designed to maximally reduce SI within the myocardium. These parameters provided an in plane spatial resolution of 0.23×0.23 mm. The inversion time (TI) for the delayed enhancement images was adjusted on the first baseline image acquisition to provide a uniform dark myocardium. This TI and the time after contrast injection used to acquire the Gd enhanced SI images (20 minutes) were kept constant at the baseline and subsequent CMR examinations for all of the animals in the study.

CMR data analysis

During acquisition, images were identified without reference to animal identifiers with a code generated prior to beginning the study. Each calculation of Gd-SI and LVEF was analyzed by an individual blinded to animal identifiers, other components of the corresponding CMR exam, and prior CMR exams of the same measure (a blinded unpaired

NIH-PA Author Manuscript

NIH-PA Author Manuscript

NIH-PA Author Manuscript

read). Random sorting of the data was performed so that the analyst was unaware of the animal's treatment (NS or DOX).

On the Gd-SI acquisitions, regions of interest (ROI) encompassing the LV myocardium on the multi-slice short acquisition were drawn by hand (Figure 1). Great care was taken to avoid including high signal intensities associated with the blood pool in the LV cavity or myocardial fat outside of the heart. The SI and location (x, y, z coordinates) of each voxel within the ROI was recorded on the Gd-SI images. In addition, a ROI was drawn separately in air on the images.[6] Values for mean Gd-SI for analysis were derived by subtracting the intensities from the mean background noise noted from the ROI within air.

Animal sacrifice and pathology data

After sacrifice, gross examination of the rats included an assessment of heart failure based upon the presence of ascites, pleural effusion, and cardiac dilation. The hearts were fixed with chilled paraformaldehyde for 24 hours and then transferred to 70% ethanol. Appropriate sections were trimmed as determined by the same landmarks used to obtain the middle short axis view on the CMR images (6 mm from the LV apex at the mid-papillary muscle level). The sections were embedded in paraffin, processed routinely for histology, cut at 4-6μm, and then stained with haematoxylin and eosin (H&E), and Masson's trichrome. All slide preparations were then examined by light microscopy. The sections were also stained by immunohistochemistry for cleaved caspase-3 according to standard methods (Cell Signaling Corporation, Danvers, MA). All sections were examined by an American College of Veterinary Pathology (ACVP) board certified veterinary pathologist in a blinded fashion. The H& E sections were examined for signs of injury, including myocellular degeneration, necrosis, edema, variation in fiber size, shape, staining, and inflammation.

Statistical analyses

By design, there were three treatment groups of animals (NS, DOX 1.5 mg/kg/wk, and DOX 2.5 mg/kg/wk) and animals within each group were measured at different numbers of time points based on the pre-specified study design (i.e., for planned animal sacrifices at specific time points). All analyses that examined changes within groups accounted for the within animal correlation by using paired t-tests, and analyses that compared groups at a fixed point in time were performed with analysis of variance or two sample t-tests for comparisons (depending upon whether the comparisons were between all 3 groups or between 2 groups). One variable, the appearance score, was a nominal variable with 5 levels (Table 1) and was compared among groups using the Kruskal-Wallis test. Only if there were overall significant differences in appearance among the 3 groups at a time point would pairwise comparisons be tested between the saline and other 2 groups. Fisher's Exact tests were used for comparing other categorical outcomes.

The first set of comparisons within groups were compared over time using paired t-tests to determine whether there were any changes in measures (heart rate, LVEF [%], and SI) over time within one of the 3 treatment groups (NS, DOX 1.5, and DOX 2.5). In addition, our NS animals served as a control population that was not exposed to DOX. Next, comparisons between groups were made to determine whether the change in SI within the LV myocardium could predict the primary outcome (referred to as EVENT-YES henceforth) or those that did not (referred to as EVENT-NO henceforth) experience a primary event.

Several different potential outcomes were then derived to see if any were related to the EVENT-YES/EVENT-NO groupings (Figure 2). Mean values for each of these measures were compared between groups (EVENT-YES/ EVENT-NO) using 2-sample t-tests. Next, receiver operating characteristics analyses were performed to determine whether a cut-point

NIH-PA Author Manuscript

NIH-PA Author Manuscript

NIH-PA Author Manuscript

could be identified for each of the 7 defined analyses that could accurately discriminate animals that would be EVENT-YES or EVENT-NO. Sensitivity and specificity estimates were then calculated for the optimal cut-points.

Comparisons were also made between groups for the histopathological findings, including necrosis, inflammation, and myofiber vacuolization using Fisher's Exact tests to see whether groups that exhibited larger LVEF changes had corresponding differences in pathological outcomes. All values are reported as mean±standard error unless stated otherwise; a p-value ≤0.05 was considered significant. For all analyses SAS Version 9.1 was used.

Results

Appearance and demographic data for the animals in the study are presented in Table 1. At baseline, the appearance was identical in the three groups while the heart rate, LVEF, and mean SI were similar amongst the groups. Also shown are the number of animals scanned, sacrificed, and experiencing an unexpected death at each time point in the study. Animals with inadequate cardiac gating (and consequent imaging artifacts) at the time of CMR were not included in the analysis. By week 2, animals receiving low or high doses of DOX showed a significantly worse appearance relative to the animals in the NS group ($p<0.0034$ from the Kruskal Wallis test for three group comparison, $p=0.0023$ for the 1.5mg/kg/wk, and $p=0.028$ for the 2.5 mg/kg/wk DOX, respectively)). The worsening appearance scores persisted at 4 weeks and beyond ($p<0.001$ at week 4 (for overall and both 2-way comparisons), $p<0.002$ at week 7 (for overall and both 2-way comparisons), and $p<0.021$ at week 10 (for overall and both 2-way comparisons).

Two weeks after receipt of DOX, the LVEF remained relatively unchanged (Table 1). At 7 weeks however, the LVEF averaged 78%±2%, 72%±3%, and 55%±6%, in the animals receiving NS, 1.5 mg/kg DOX, and 2.5 mg/kg DOX, respectively (Table 1). As shown in Figure 3, of the animals receiving 1.5 mg/kg of DOX, 6 of 19 experienced a primary event (3 developed a LVEF drop <65% and 3 died unexpectedly overnight). Of the 14 animals receiving 2.5 mg/kg of DOX, 10 experienced a primary event: all with a substantial drop in LVEF.

As shown in Table 2, the LVEF was similar as baseline and at 2 weeks in animals receiving NS, DOX without a primary event, and DOX with a primary event. Relative to the baseline values, the LVEF remained relatively constant throughout the study in NS animals and those receiving DOX without an event. In the animals receiving DOX with an event, an initial small change (not meeting the criteria for a cardiac event) in LVEF occurred relative to baseline at 2 weeks (74±2% at baseline and 70±1% at 2 weeks, $p=0.05$).

The mean SI averaged 5.3±1.8, 3.0±1.0, and 6.0±1.4 at baseline in animals receiving NS, 1.5 mg/kg DOX, and 2.5 mg/kg DOX, respectively. Throughout the experiment, the average SI did not exceed 1 standard deviation of the baseline value at the 2, 4, 7, or 10-week interval in the animals receiving NS (Table 2). The average SI in the animals receiving 1.5 mg/kg of DOX also did not increase by more than 1 standard deviation in value from the baseline measure until the 7^{th} week of the experiment. In the animals receiving 2.5 mg/kg of DOX, the SI increased to 12.8±5.1, at the 2-week sample point and further thereafter to a value of 28.3±8.1. In animals receiving the 2.5 mg/kg of DOX, the SI was significantly higher than the SI observed in the other 2 groups, as well as the SI relative to baseline ($p<0.05$ for all comparisons).

For those animals that experienced a primary event (Table 2), the mean SI at 7 weeks was higher compared to either the animals receiving DOX that did not experience a primary event ($p= 0.02$), or the animals receiving NS ($p=0.03$). At the time of the drop in LVEF, the

NIH-PA Author Manuscript

NIH-PA Author Manuscript

NIH-PA Author Manuscript

mean Gd-SI was 33.5±5.2 versus 6.6±3.2 in animals that did not experience a primary event (p=0.0001). The difference in SI in those experiencing a primary event versus the combined NS and animals receiving DOX without an event was high (p=0.004). Relative to the NS controls and the animals receiving DOX that did not experience a primary event, the average SI at 2 weeks significantly increased in the animals that subsequently experienced a primary event later in the study (p=0.03). Examples of histograms from animals demonstrating receipt of NS versus those animals receiving DOX with and without a cardiac event are shown in Figure 4.

To determine if measures of Gd enhanced SI could be used to predict future primary events (a measure of potential clinical utility), measures of Gd-SI from exams prior to events were assessed relative to baseline measures, as well as measures obtained from the preceding intermediate period (Figure 2). In the animals with an event, the mean signal intensities at the measurement point prior to the event averaged 22.3±3.5 vs. 3.0±2.9 in animals without an event (p<0.0001). In these same animals with and without events, when the difference between the measurement point Gd-SI prior to the event was compared to the measurement at a point in time two intervals before the event, the mean difference in SI was 14.8±5.4 in the animals that experienced an event versus 2.3±4.3 in animals without an event (p=0.098).

The change from baseline in Gd-SI to the measurement point prior to a primary event was 17.0±3.8 versus 0±3.2 in animals without a primary event (p=0.0009). Similarly, the change in SI over time was equally different between the sample point in measurements prior to the primary event versus baseline relative to animals without a primary event (p=0.0007). Results were similar after accounting for the time intervals associated with these changes occurring relative to baseline (p=0.001 for both intervals 6 and 7 in Figure 2).

We did not perform a formal test/retest assessment of the SI measurements, however we examined the change from baseline for all NS animals and found that the average difference was 2.58 with a standard deviation of 4.5, indicating that there is some variability in this measure with “healthy” animals over time. When we examined the magnitude of the changes seen in the DOX treated animals, the observed change in SI was several fold larger than the standard deviation of SIs found in NS animals. In fact, the effect is nearly 5 times as large as the standard deviation for the change in SI across all NS measures.

A receiver operating curve was generated to determine the optimal times to assess characteristics in SI at time points prior to an event that would forecast a future event. As shown in Figure 5, a value in SI >8.2 in a prior sample period was predictive of a future cardiac event. This remained true even if one excluded the 3 unexpected deaths and only assessed LVEF drop. Similarly, an increase in SI of >1.0 between 2 exams prior to an event, or an increase in SI >2.9 from baseline were also predictive of an event.

To investigate potential etiologies associated with increased SI, histopathologic examination of the heart was accomplished in sections from which the imaging planes were selected to obtain the data for the study. As shown in Figure 6, there was no significant increase in fibrosis, myocellular death, or apoptosis among the hearts of animals experiencing a drop in LVEF compared to those animals that did not. Importantly however, clear intracytoplasmic myocellular vacuoles and variation in myofiber size and tinctorial quality was present regularly in animals with a drop in LVEF and an increase in CMR SI (Figures 4 and 6). These findings are consistent with vacuolar degeneration resulting from intracellular edema.[12] None of the animals without a change in Gd-SI developed myocellular degeneration.

NIH-PA Author Manuscript

NIH-PA Author Manuscript

NIH-PA Author Manuscript

Discussion

This study has 4 important conclusions: first, the mean voxel intensity within the LV myocardium obtained on GEIR imaging 20 minutes after the administration of Gd increases in animals that experience a deterioration in LVEF after receipt of DOX. Second, the increase in mean SI within the LV myocardium after Gd that occurs during receipt of DOX occurs prior to, and thus forecasting, a future clinically important drop in LVEF. Third, animals that do not experience a drop in LVEF or an unexpected death after receipt of DOX do not experience an increase in SI within the LV myocardium after Gd. Fourth, animals that drop their LVEF and experience an early increase in Gd-SI after receipt of DOX exhibit myocellular vacuolization, a phenomenon previously described histopathologically after DOX.

The imaging strategy utilized in this study enabled us to assess the utility of serial MR measures and their relationship to important adverse cardiac outcomes in animals receiving DOX. As shown in Table 2, animals experiencing a primary event also exhibited an increase in Gd-CMR SI as the LVEF dropped. This underlying marker of change in tissue characteristics has the potential for future clinical use to identify the presence or absence of DOX cardiotoxicity in cancer patients that may experience a change in LVEF for reasons other than DOX toxicity (volume depletion, infection, etc.). As shown in Figures 2 and 5, we were able to utilize our data to generate receiver operating curves demonstrating several metrics that may be useful in future studies for identifying characteristics of CMR SI change that forecast future adverse events related to DOX administration. In addition, when serial measures of T1-weighted signal characteristics did not change, the animal's LVEF remained preserved and no adverse events occurred (Table 2).

The method of analysis of the Gd enhanced images used in this study differs from those used previously to identify myocellular injury after a myocardial infarction (MI) in which myocellular injury is defined in voxels with a SI >2 standard deviations above background intensity within non-enhanced LV myocardium.[6] Methods that visualize well circumscribed myocardial infarcts are not well suited for a process that causes diffuse cardiac injury throughout the heart. To overcome this limitation, we developed a method to determine the mean voxel intensity of all the voxels within the short axis slice of the left ventricle (Figure 1). This method evaluates a process that may involve the LV myocardium in a global, more randomly distributed pattern.

Our study incorporated histopathologic correlation with the CMR findings, thereby allowing investigation of the possible reasons for the increases in SI. Previously, heightened SI with delayed enhancement Gd-CMR has been considered the result of myocardial necrosis and fibrosis. In fact, we hypothesized fibrosis would be the etiology of events in this study.[13] Importantly however, Masson's trichrome staining confirmed an absence of fibrosis in the hearts of our animals.

Histopathologically, there was no or little fibrosis, substantial necrosis, or apoptosis in our specimens, thus, the vacuolar degeneration, an indication of intracellular edema, seems the most likely cause for the increased CMR signal intensity observed in this study. As cells become dysfunctional with membrane damage, there are osmotic imbalances that cause water to accumulate within them. With early cellular injury, Gd could also accumulate extracellularly due to cellular disarray without cellular destruction. Since Gd, an intra and extracellular contrast agent, changes the relativity of the water in spaces where it has accumulated, the SI on our T1-weighted images would therefore increase.[13] Interestingly, recent data have demonstrated the utility of T2-weighted imaging (highly sensitive to water accumulation without the need for contrast administration) in various forms of

NIH-PA Author Manuscript

NIH-PA Author Manuscript

NIH-PA Author Manuscript

cardiomyopathy due to inflammation.[5] Our particular study design did not allow us to acquire T2-weighted images; however, given our histopathologic findings suggestive of myocardial intra- and extracellular water accumulation, further investigation of T2-weighted imaging methods in DOX cardiotoxicity is warranted.

The imaging technique utilized in this study was based on the selection of a consistent TI throughout the study. This allowed us to appreciate differences in SI relative to the baseline condition. Practically, however, this technique requires precise timing of image acquisition relative to contrast administration. Also, the magnet surface coil arrangement, shim, and pre-scan parameters must be relatively constant on successive examinations. In longitudinal human studies, these conditions could be difficult to achieve. Recently, T1-mapping strategies have been reported for identification of processes that affect the myocardium in a diffuse pattern;[14,15] these T1-weighted mapping strategies may be of use and also warrant further study.

Over the past 25 years, 3 other studies (2 in animals and 1 in humans) have demonstrated an association between increased T1 relaxation and DOX cardiotoxicity. In the 2 animal studies, excised myocardial tissue exposed to DOX was found to have increased T1-relaxation measured with inversion recovery pulse sequences or nuclear magnetic resonance spectroscopy.[16,17] In human subjects, increased early relative enhancement (as measured with T1-weighted images in the first 2 minutes after Gd contrast administration) was associated with future CHF after DOX.[18] The current study contributes to these studies in that it (1) confirms that changes in SI on T1-weighted images are associated with DOX cardiotoxicity, (2) demonstrates that an absence of change in SI on T1-weighted images is associated with a preservation of LVEF after receipt of DOX, and finally (3) identifies a histopathological correlate of DOX toxicity in animals that drop their LVEF and experience an increase in T1-weighted SI within the LV myocardium.

A small decrement in LVEF was observed at the 2-week time interval in animals that developed a primary event (Table 2). Detection of a small change in LVEF was possible in this study due to the high reproducibility and accuracy of three-dimensional CMR techniques.[8,10] The 3-dimensional CMR assessment of LV volumes and LVEF, have been shown previously to be able to appreciate 3% changes in LVEF after an intervention.[8]

Our study has limitations. First, we did not include animals with existing LV dysfunction. Animals with existing cardiomyopathies may have abnormal resting SIs for which our imaging strategy could have lower utility. Second, our CMR methodology required precise selection TIs and coordination of image acquisition after Gd-contrast administration. This level of precision could be difficult to replicate in a busy clinical private outpatient or hospital based CMR center. Further studies that involve strategies that would not necessarily require specific TIs but could account for differences in imaging conditions over time, such as T1 mapping, may have greater utility. Third, our study design correlated CMR T1-weighted image SI changes with histopathology; animals were therefore sacrificed relatively early in the course of DOX administration. CMR correlations with more advanced cardiac injury were not obtained, nor did we assess whether the early lesions would reverse after discontinuation of DOX. Fourth, anthracyclines, such as DOX, have been shown to cause nephrotoxicity due to oxidative stress. In this study, we have no histopathological data from the kidneys of the animals, and therefore, we are uncertain whether potential renal damage influenced animal outcomes in the study.[19] Finally, we utilized a Sprague-Dawley animal model of cardiotoxicity that exhibits genetic variability and thus less susceptibility to cardiotoxicity after DOX exposure. Other animals including canines,[20] non-human primates,[20] or mice[20] have been shown highly susceptible to DOX and may be useful in future studies.

NIH-PA Author Manuscript

NIH-PA Author Manuscript

NIH-PA Author Manuscript

In conclusion, we demonstrate that changes in SI within the LV myocardium on T1-weighted Gd enhanced images identify animals that develop future adverse cardiac events (primarily a fall in LVEF) after doxorubicin. In animals without a change in T1-weighted SI after Gd, adverse cardiac events do not occur. Early changes in Gd-SI are associated with intracellular vacuolization, an indication of myocellular degeneration consistent with DOX cardiotoxicity. The results of this study and others suggest that future human studies should be performed to determine the role of CMR for detecting doxorubicin cardiotoxicity and preventing CHF in patients treated for cancer.

Acknowledgments

We acknowledge the expertise of Deanna Carr, who assisted in preparation of the manuscript.

Sources of Funding

This work was supported by National Institute of Health Grants R21CA109224, R33CA12196, and a grant from the Susan G. Komen Foundation (BCTR07007769).

References

1. Hortobagyi GN. Treatment of breast cancer. N Eng J Med. 1998; 339:974–984.
2. Leandro J, Dyck J, Poppe D, Shore R, Airhart C, Greenberg M, Gilday D, Smallhorn J, Benson L. Cardiac dysfunction late after cardiotoxic therapy for childhood cancer. Am J Cardiol. 1994; 74:1152–6. [PubMed: 7977077]
3. Gottdiener JS, Mathisen DJ, Borer JS, Bonow RO, Myers CE, Barr LH, Schwartz DE, Bacharach SL, Green MV, Rosenberg SA. Doxorubicin cardiotoxicity: assessment of late left ventricular dysfunction by radionuclide cineangiography. Ann Intern Med. 1981; 94:430–5. [PubMed: 7212498]
4. Doyle JJ, Neugut AI, Jacobson JS, Grann VR, Hershman DL. Chemotherapy and cardiotoxicity in older breast cancer patients: A population-based study. J Clin Oncol. 2005; 23:8597–605. [PubMed: 16314622]
5. DeVita, V,T. 4th ed. Lippincott; Philadelphia, Pennsylvania: 1993. Cancer Principles and Practice of Oncology.
6. Kim RJ, Wu E, Rafael A, Chen EL, Parker MA, Simonetti O, Klocke FJ, Bonow RO, Judd RM. The use of contrast-enhanced magnetic resonance imaging to identify reversible myocardial dysfunction. N Engl J Med. 2000; 343:1445–53. [PubMed: 11078769]
7. Hundley WG, Kizilbash AM, Afridi I, Franco F, Peshock RM, Grayburn PA. Administration of an intravenous perfluorocarbon contrast agent improves echocardiographic determination of left ventricular volumes and ejection fraction: comparison with cine magnetic resonance imaging. J Am Coll Cardiol. 1998; 32:1426–32. [PubMed: 9809958]
8. Chuang ML, Hibberd MG, Salton CJ, Beaudin RA, Riley MF, Parker RA, Douglas PS, Manning WJ. Importance of imaging method over imaging modality in noninvasive determination of left ventricular volumes and ejection fraction: assessment by two- and three-dimensional echocardiography and magnetic resonance imaging. J Am Coll Cardiol. 2000; 35:477–84. [PubMed: 10676697]
9. Hundley WG, Li HF, Willard JE, Landau C, Lange RA, Meshack BM, Hillis LD, Peshock RM. Magnetic resonance imaging assessment of the severity of mitral regurgitation. Comparison with invasive techniques. Circulation. 1995; 92:1151–8. [PubMed: 7648660]
10. Martin ET, Fuisz AR, Pohost GM. Imaging cardiac structure and pump function. Cardiol Clin. 1998; 16:135–60. [PubMed: 9627754]
11. Gerber BL, Rochitte CE, Bluemke DA, Melin JA, Crosille P, Becker LC, Lima JA. Relation between Gd-DTPA contrast enhancement and regional inotropic response in the periphery and center of myocardial infarction. Circulation. 2001; 104:998–1004. [PubMed: 11524392]
12. Olson HM, Young DM, Prieur DJ, LeRoy AF, Reagan RL. Electrolyte and morphologic alterations of myocardium in adriamycin-treated rabbits. Am J Pathol. 1974; 77:439–54. [PubMed: 4432914]

NIH-PA Author Manuscript

NIH-PA Author Manuscript

NIH-PA Author Manuscript

13. Choi KM, Kim RJ, Gubernikoff G, Vargas JD, Parker M, Judd RM. Transmural extent of acute myocardial infarction predicts long-term improvement in contractile function. Circulation. 2001; 104:1101–7. [PubMed: 11535563]

14. Ferrans VJ. Overview of cardiac pathology in relation to anthracycline cardiotoxicity. Cancer Treat Rep. 1978; 62:955–61. [PubMed: 352510]

15. Messroghli DR, Niendorf T, Schulz-Menger J, Dietz R, Friedrich MG. T1 mapping in patients with acute myocardial infarction. J Cardiovasc Magn Reson. 2003; 5:353–9. [PubMed: 12765114]

16. Thompson RC, Canby RC, Lojeski EW, Ratner AV, Fallon JT, Pohost GM. Adriamycin cardiotoxicity and proton nuclear magnetic resonance relaxation properties. Am Heart J. 1987; 113:1444–9. [PubMed: 3591613]

17. Cottin Y, Ribuot C, Maupoil V, Godin D, Arnould L, Brunotte F, Rochette L. Early incidence of adriamycin treatment on cardiac parameters in the rat. Can J Physiol Pharmacol. 1994; 72:140–5. [PubMed: 8050054]

18. Wassmuth R, Lentzsch S, Erdbruegger U, Schulz-Menger J, Doerken B, Dietz R, Friedrich MG. Subclinical cardiotoxic effects of anthracyclines as assessed by magnetic resonance imaging-a pilot study. Am Heart J. 2001; 141:1007–13. [PubMed: 11376317]

19. Yilmaz S, Atessahin A, Sahna E, Karahan I, Ozer S. Protective effect of lycopene on adriamycin-induced cardiotoxicity and nephrotoxicity. Toxicology. 2006; 218:164–71. [PubMed: 16325981]

20. Herman EH, Ferrans VJ. Animal models of anthracycline cardiotoxicity: Basic mechanisms and cardioprotective activity. Progress in Pediatric Cardiology. 1998; 8:49–58.

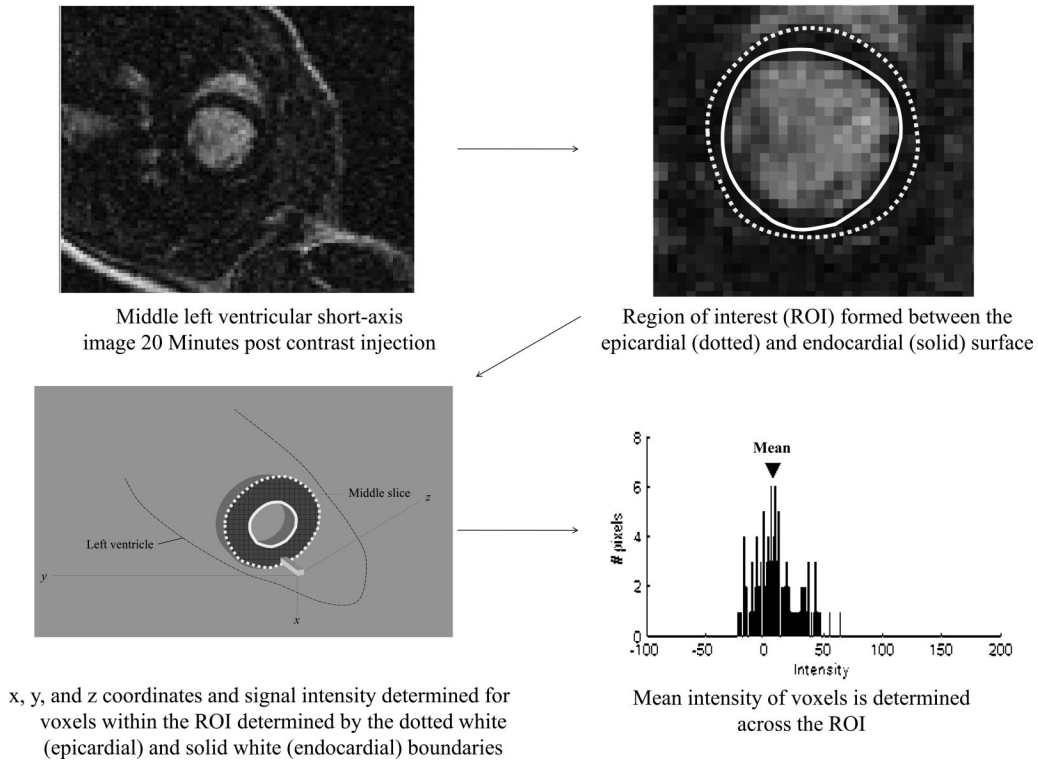

Figure 1. Left ventricular (LV) myocardial signal intensity

In the top left, a middle LV short axis image obtained 20 minutes after gadolinium contrast. As shown, the LV myocardial cavity is white and the LV myocardium is dark. On this short axis image, a region of interest was identified (top right) bounded by the LV endocardial surface (solid line) and the LV epicardial surface (dotted line). Within this region of interest the x, y, and z coordinates along with the signal intensity for all the boxes were recorded (bottom left). The number of voxels along with their intensity was plotted and the mean voxel intensity was determined (bottom right). This value was then subtracted from the background noise to obtain the mean voxel intensity.

NIH-PA Author Manuscript NIH-PA Author Manuscript NIH-PA Author Manuscript

NIH-PA Author Manuscript

NIH-PA Author Manuscript

NIH-PA Author Manuscript

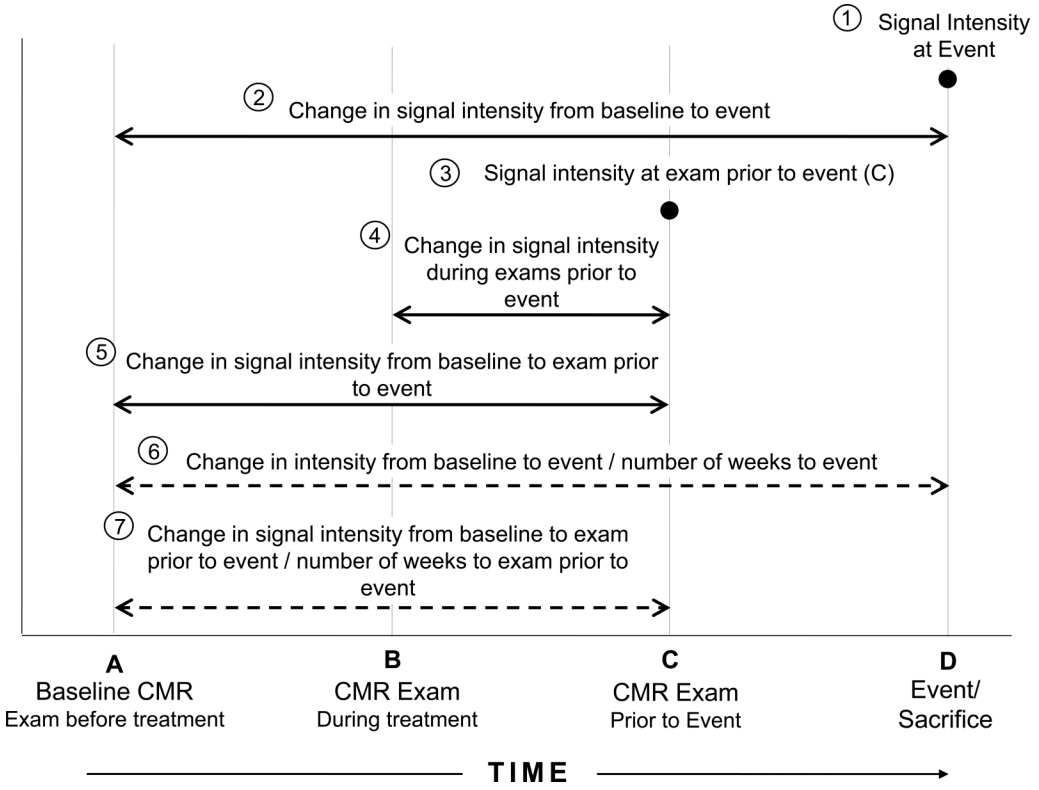

Figure 2. Gadolinium CMR sample points and intervals

Longitudinal study design showing the multiple sample points and intervals for assessing the relationship between signal intensity and left ventricular ejection fraction measures. For animals not experiencing events, the last point in time sampled for the animal served as their final sample point (labeled D on the Figure).

Figure 3. Study Design

As shown 7, 19, and 14 animals were initiated into this study in groups receiving normal saline, 1.5 mg/kg/week of doxorubicin, and 2.5 mg/kg/week of doxorubicin, respectively. Upon animal sacrifice, 24 animals had not experienced a primary event and 16 animals experienced a primary event (13 with a drop in LVEF; 3 with sudden death)

NIH-PA Author Manuscript
NIH-PA Author Manuscript
NIH-PA Author Manuscript

Figure 4. Serial histograms and histopathology

On the top portion of the Figure, 4 week histograms of the number of pixels (y-axes) and intensities (x-axes) in individual animals after receipt of saline (top left), doxorubicin without (top middle) and with (top right) an ejection fraction (EF) drop. On the right are 40-power haematoxylin and eosin (H&E) histopatholigic images from the same animals. As shown, mean intensity increased in the animals that dropped their EF corresponding to vacuolization (arrows bottom right H&E).

NIH-PA Author Manuscript
NIH-PA Author Manuscript
NIH-PA Author Manuscript

Figure 5. Prediction of future primary events

Receiving operator characteristic curves to determine the cutoff point for: (1) the signal intensity (SI) of the point prior to a primary event (Gd-PRIOR to EVENT; dotted line); (2) the change in SI from the 2 examinations prior to the primary event (Gd-INTERMEDIATE; dashed line); and (3) the change in SI from baseline to the point prior to the primary event (Gd-BASELINE to PRIOR EVENT; dash/dot line). As shown, changes in SI early in the study predicted future events.

NIH-PA Author Manuscript
NIH-PA Author Manuscript
NIH-PA Author Manuscript

NIH-PA Author Manuscript

NIH-PA Author Manuscript

NIH-PA Author Manuscript

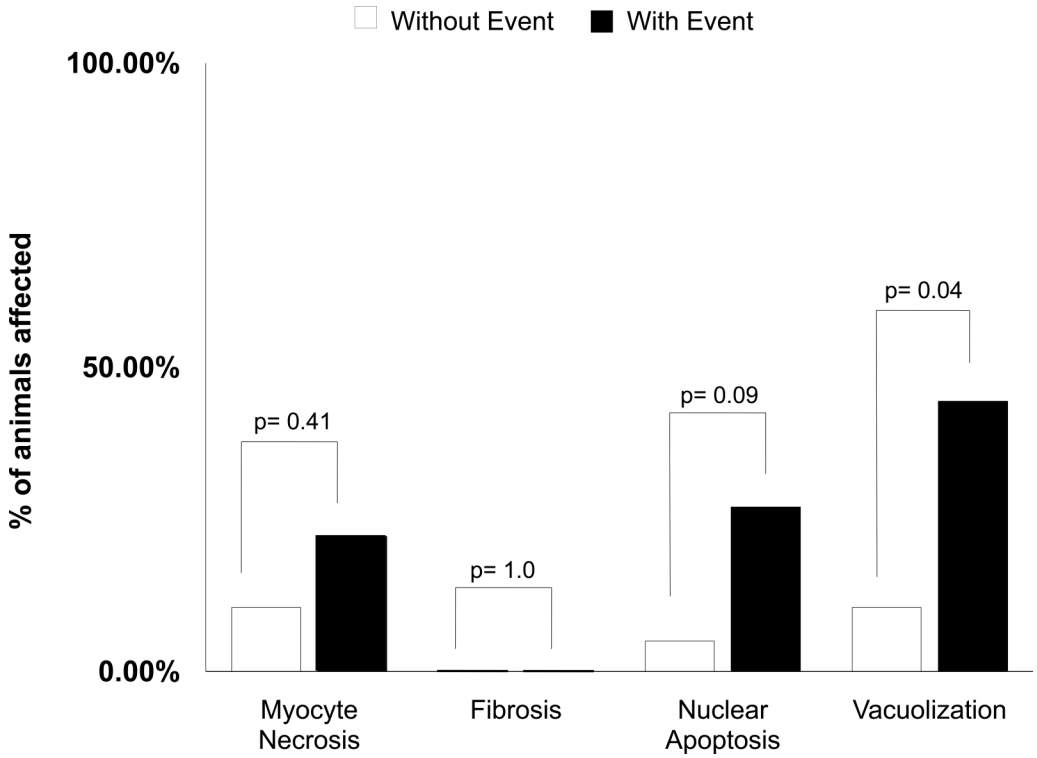

Figure 6. Myocardial morphology

Bar graph displaying the percentage of animals which developed myocellular necrosis, fibrosis, apoptosis, and vacuolar degeneration. Animals experiencing the primary endpoint of death (n=3) or drop in left ventricular ejection fraction (n=13) exhibited more vacuolization relative to animals that did not experience these primary endpoints.

NIH-PA Author Manuscript
NIH-PA Author Manuscript
NIH-PA Author Manuscript

Circ Cardiovasc Imaging. Author manuscript; available in PMC 2011 September 1.

Table 1

Study Animals

Treatment	Surviving Animals	Acceptable Gating during Image Acquisition	Sacrificed for Histopathology	Unexpected Death	Appearance	LVEF (MN±SE)	Signal Intensity (MN±SE)
Normal Saline (n=7)							
0 wks	7	7	0	0	7/0/0/0/0	77±3	5.3±1.8
2 wks	7	5	1	0	6/0/1/0/0	73±2	2.4±1.3
4 wks	6	6	0	0	6/0/0/0/0	77±3	1.8±1.6
7 wks	6	5	0	0	6/0/0/0/0	78±2	3.1±3.1
10 wks	6	4	6	0	6/0/0/0/0	77±2	3.8±1.5
Doxorubicin 1.5 mg/kg (n=19)							
0 wks	19	19	0	0	19/0/0/0/0	77±1	3.0±1.0
2 wks	19	17	5	1	1/16/2/0/0	75±1	3.1±1.0
4 wks	13	10	2	0	0/11/1/0/1	75±2	3.9±1.4
7 wks	11	10	5	4	0/0/7/1/3	72±3	22.4±7.7
10 wks	2	2	2	0	0/0/1/1/0	67±9	21.7±17.3
Doxorubicin 2.5 mg/kg (n=14)							
0 wks	14	14	0	0	14/0/0/0/0	73±2	6.0±1.4
2 wks	14	12	0	0	3/11/0/0/0	70±2	12.8±5.1
4 wks	14	14	9	1	0/1/10/2/1	66±3*	28.3±8.1*
7 wks	4	4	3	0	0/0/1/2/1	55±6	26.3±7.9
10 wks	1	1	1	0	0/0/1/0/0	74± n/a	5.8± n/a

Appearance score: numbers of animals with respective appearance scores of 1/2/3/4/5, where 1=excellent: active, eating/drinking; 2=good: active, slight hair loss; 3=fair: less active, slight bloating; 4=poor: reluctant to move, poor appetite and pallor, diarrhea; 5=critical: marked pallor, not eating/drinking

Abbreviations: LVEF=left ventricular ejection fraction, MN=mean, SE=standard error

*p<0.05 from 0 weeks

NIH-PA Author Manuscript

NIH-PA Author Manuscript

NIH-PA Author Manuscript

Table 2

LVEF and signal intensity in animals with and without events (mean±standard error)

Treatment	Acceptable gating (n)	LVEF (%)	Signal Intensity
Normal Saline			
0 wks	7	77±3	5.3±1.8
2 wks	5	73±2	2.4±1.3
4 wks	6	77±3	1.8±1.6
7 wks	5	78±2	3.1±3.1
Doxorubicin: No Drop/Event			
0 wks	17	77±1	3.3±1.1
2 wks	15	76±1	6.8±3.3
4 wks	8	78±3	8.3±0.4
7 wks	5	77±3	2.2±0.4
Doxorubicin: Yes Drop/Event			
0 wks	16	74±2	5.3±1.4
2 wks	14	70±1*	7.1±3.1
4 wks	16	65±2*	23.7±8.2
7 wks	9	61±4*	29.4±5.0*

Abbreviations: LVEF=left ventricular ejection fraction

* $p<0.05$ from 0 weeks